Grape Seed Extract-Soluplus Dispersion and its Antioxidant Activity

R. Rajakumari [a, b], Tatiana Volova[b], Oluwatobi Samuel Oluwafemi*[c, d], Rajesh Kumar[e], Sabu Thomas[a, f] and Nandakumar Kalarikkal*[a, g]

[a]*International and Inter-University Centre for Nanoscience and Nanotechnology, Mahatma Gandhi University, Kerala, 686560, India*

[b]*Siberian Federal University, 79 Svobodnyi Av., Krasnoyarsk, 660041, Russia*

E-mail: volova45@mail.ru

[c] *Department of Chemical Sciences, University of Johannesburg, South Africa*

[d]*Centre for Nanomaterials Sciences Research, University of Johannesburg, Johannesburg, South Africa*

E-mail: oluwafemi.oluwatobi@gmail.com

[e]*Department of Pharmacology, Saveetha Dental College and Hospitals, Saveetha Institute of Medical and Technical Sciences (SIMATS), Chennai, 600077, Tamilnadu, India*

E-mail: ssrajeshkumar@hotmail.com, Tel: +91 96297 39263

[f]*School of Chemical Sciences, Mahatma Gandhi University, Kerala, 686560, India.*

E-mail: sabuchathukulam@yahoo.co.uk, Fax: +91-481-2731002, Tel: +91-481-2731002

[g]*School of Pure and Applied Physics, Mahatma Gandhi University, Kerala, 686560, India.*

E-mail: nkkalarikkal@mgu.ac.in, Fax: +91-481-2731669, Tel: +91-481- 2731669

**Corresponding Authors E mail: oluwafemi.oluwatobi@gmail.com;*

nkkalarikkal@mgu.ac.in

Abstract

Objective

The main objective of this work was to formulate a nanodispersion containing grape seed extract and analysed its release profile, antioxidant potential of the prepared formulations.

Methods

The grape seed extract (GSE) containing proanthocyanidins (PC's) has been dispersed in polymer matrix soluplus (SOLU) by the freeze-drying method. The morphological analysis was carried out using atomic force microscopy (AFM), scanning electron microscopy (SEM) and Transmission electron microscopy (TEM). The *in-vitro* release of the nanodispersion formulations was evaluated by simulated intestinal fluid (SIF). The antioxidant activity of GSE and the formulation were evaluated by employing various *in-vitro* assays such as 2, 2'-azino-bis (3-ethylbenzothiazoline-6-sulphonic acid) (ABTS), 2, 2-diphenyl-1- picrylhydrazyl (DPPH), Ferric reducing antioxidant power (FRAP) and peroxidation inhibiting activity.

Results

The formulation FIII (1:5) resulted in a stable formulation with a higher loading efficiency of 95.36 %, a particle size of 69.90 nm, a polydispersity index of 0.154 and a zeta potential value of -82.10 mV. The antioxidant efficiency of GSE-SOLU evaluated by DPPH was found to be 96.7 %. The ABTS and FRAP model exhibited a dose-dependent scavenging activity. Linoleic model of FIII formulation and GSE exhibited a 66.14 and 86.58 % inhibition respectively at 200 µg/l.

Conclusions

The main reason for excellent scavenging activity of the formulations can be attributed to the presence of monomeric, dimeric, oligomeric procyanidins and the phenolic group. The present work denotes that GSE constitutes a good source of PC's and will be useful in the prevention and treatment of free radical related diseases.

Key Words: Grape seed extract; Proanthocyanidins; Antioxidant; Soluplus; Freeze-drying; Dispersion

1. Introduction

Many diseases are as a result of oxidative stress on the cells due to the release of free radicals. The reactive oxygen species (ROS) are superoxide anion, hydroxyl radicals, hydrogen peroxide and singlet oxygen were said to be different forms of free radicals [1]. Therefore, antioxidative defence system is necessary to act against the free radicals production (Fig 1). Moreover, the damage on cells due to free radicals causes several chronic diseases such as cancer, arthritis, atherosclerosis, wound, neurodegenerative diseases and diabetes mellitus [2, 3]. For this reason, antioxidants are commonly used in the treatment and prevention of chronic diseases.

Currently, the use of natural therapeutics based on nanotechnology in healthcare is greatly utilised in areas such as drug delivery, imaging, rapid diagnosis, tissue regeneration and development of new therapeutics [4–7]. The preparation of the green synthesis of nanodispersion is growing into a key approach in nanotechnology. Proanthocyanidins (PCs) are a class of polyphenols and chemically, they are oligomeric flavonoids found in a variety of plants. It is an important constituent found in varying concentrations in GSE and the antioxidant activity of PCs are higher than the widely used antioxidant molecules such as ascorbic, trolox and rutin. This is because of the position of the hydroxyl groups in the PCs [8, 9]. The flavonoids are quickly hydrolysed in the intestine by bacteria to generate aglycones which are then metabolized into phenylacetic, phenylpropionic, and phenylvaleric form of PCs. They are retained in the large intestine after an oral intake and are found not to be stable which is probably due to damage of the C-ring of proanthocyanidins [10, 11].

Apart from antioxidant activity, PCs shows anticancer [12], antidiabetic [13], anti-inflammatory [14] and antibacterial activities [15]. Despite the extensive range of pharmacological properties, the usage of PCs in pharmaceutical arena is very limited owing to its poor bioavailability, poor permeability and poor stability in a biological medium [16]. Therefore to circumvent the problems, PCs are entrapped/adsorbed into a biodegradable polymer. Recently, SOLU is widely used as a biodegradable polymer for many therapeutically active moieties due to its amphiphilic nature, biocompatibility, low toxicity, good mechanical strength and controlled release [17]. Selection of a proper carrier is a significant step in the formulation of nano dispersions containing compounds with low permeability and high molecular weight. Soluplus has polyvinyl caprolactam (PVC) (57 % vinyl caprolactam) – polyvinyl acetate (PVA) (30 %) – polyethylene glycol (PEG) graft copolymer vinyl acetate). SOLU carrier is one of the 4^{th} generation of dispersions proposed in enhancing the stability of the formulation [18]. It is reported that SOLU efficiently increase the absorption of the low permeable molecules when used as a drug carrier [19]. SOLU improved the dissolution of the low bioavailable molecules by electrospinning and extrusion technology [20]. It is also reported that PC molecule has been incorporated into liposomes and nanoparticles [21] but in-depth characterisations of PCs are not reported.

In this study, proanthocyanidin molecule was dispersed into SOLU by the freeze-drying method. The GSE-SOLU dispersion was characterised by atomic force microscope (AFM), scanning electron microscope (SEM) and transmission electron microscope (TEM). The antioxidant activity was carried out to enhance its application in the food and Pharmaceutical industries. PCs dispersed in the SOLU matrix showed a controlled release behaviour indicating that the PCs dispersed SOLU may improve bioavailability and stability of PCs. The addition of SOLU in GSE retards oxidative spoilage and extends the shelf life of formulation. Moreover, this study provides better insights of GSE-SOLU as an effective antioxidant compound in food

and Pharmaceutical industries. The higher antioxidant activity in formulations is attributed to the SOLU which is used to scavenge or drain radicals that are harmful. This property of SOLU incorporated GSE molecule paved way for dispersing various antioxidant moieties for developing better therapeutic compounds.

2. Materials and Methods

Polyethylene glycol-polyvinyl acetate-polyvinyl caprolactam (Soluplus) were received from BASF Corporation, Mumbai. GSE (Proanthocyanidins) from JF Naturals, China. DPPH, ABTS, Linoleic acid, potassiumpersulphate, potassium ferric cyanide, Aluminum chloride, Ferrozine, Ferric chloride were obtained from Sigma Chemicals (Mumbai). The solvents used in this study were of analytical grade purchased from E-Merck (Mumbai).

2.1 *Lyophilisation*

The different ratios of GSE-SOLU (1:1 (FI), 1:3 (FII), 1:5 (FIII), 1:7 (FIV)) were dissolved in water and the prepared aqueous solution was dispersed using magnetic stirrer at 125 rpm for 30 min. Then, the dispersion was sonicated for about 10 mins at room temperature and it was frozen at −45 °C. Finally, the frozen sample was subjected to lyophilisation at −84 °C with a pressure of 7×10^{-2} mbar for 12 h using freeze-dryer (Sub-Zero, USA) to obtain the dried solid.

2.2 *Optimization of GSE loading*

GSE-SOLU was prepared using different loadings such as 1 %, 3 %, 5 % and 7 % of the SOLU to estimate the percentage of GSE in the soluplus matrix and the changes in the particle size, polydispersity index, zeta potential and loading of GSE-SOLU. The stirring time, sonication time and aqueous ratio were kept constant.

2.3 *Loading efficiency (LE)*

The content of GSE dispersed in SOLU was estimated by membrane filter method. GSE-SOLU (0.5 ml) was filtered through the membrane (0.22-μm), whereas the undispersed GSE was retained. The filtrate containing GSE-SOLU was mixed with methanol and determined the dispersed GSE content by HPLC (high-performance liquid chromatography) assay method. The experiments were done three times to ensure optimal loading.

2.4 *Fourier transform infrared spectroscopy (FT-IR)*

The infrared spectrum of the polymer SOLU, GSE and lyophilized GSE-SOLU (FIII) formulations were analysed using FT-IR spectrometer (Perkin Elmer). The potential interactions among the GSE and the SOLU are analysed in the solid form with a frequency of 4000-400 cm^{-1}.

2.5 *Powder X-ray diffraction*

X-ray diffraction (XRD - D8- Bruker, Germany) with the wavelength of 1.5405980 Å using Cu-kα1 radiation were used to study the diffraction patterns and crystal structures of GSE, SOLU and GSE-SOLU nanodispersion formulations.

2.6 *Distribution of particle size and zeta potential measurements*

Particle size, zeta potential and poly dispersity index (PDI) of GSE-SOLU were determined by nano zetasizer (Horiba Instruments, UK). The GSE-SOLU formulations, GSE, SOLU were dispersed in distilled water for analysis. Cumulative percentage of particle size and PDI were obtained using the Horiba software. All experiments were repeated three times.

2.7 *Morphological analysis*

2.7.1 *Atomic force microscopy (AFM) analysis*

The experiments were performed using A.P.E.R research nanotechnology instrument (Italy) in contact mode imaging method. The samples were diluted with deionized water and a drop of all the samples was placed separately over the silica wafers surface and dried. After drying, the samples were subjected to AFM analysis.

2.7.2 *Scanning electron microscopy (SEM) analysis*

The morphologies of GSE, SOLU and the GSE-SOLU formulations were obtained by Jeol-JSM-5300 scanning electron microscope (Tokyo, Japan). The samples were placed on the glass stump with double-sided adhesive tape and they are gold coated prior to analysis. Different magnifications of the images were obtained to study the morphology of the formulations.

2.7.3 *Transmission electron microscopy (TEM) analysis*

The morphology of SOLU, GSE, GSE-SOLU solid dispersions was also analysed by transmission electron microscopy (JEOL Model-JEM2100). The samples were diluted with deionized water and a drop of all the samples was individually placed on the grid and dried prior to analysis. Then, the samples were subjected to TEM analysis.

2.8 In-vitro release

The *in-vitro* release of GSE from SOLU was evaluated by simulated intestinal fluid (SIF), water and water-ethanol mixture. The procedure of Wang et al's was followed to prepare the SIF which consists of trypsin - 10 g/l, NaCl - 9 g/l, pancreatin - 10 g/l and bile salts - 3 g/l and this solution was adjusted to a pH of 6.8 [22]. The SIF was kept at 37 °C for incubation and stirred with a magnetic stirrer continuously. The solution (1 ml) was withdrawn at different time intervals of 1 h for the first 6 h, then every 3 h for the next 6h and every 8 h for 48 h. They

were centrifuged at a rotational speed of 14,000 rpm for 5 min and filtered using Millipore paper (0.45 μm). Finally, the PCs content in GSE was estimated by Waters HPLC. The mobile phase used was acetone/water/acetic acid (70/29.5/0.5 v/v/v) and stationary phase was silica column (5 μm, 250 × 4.6 mm). Standard and sample were injected separately and the components eluted was detected by spectrometer. The peaks were quantified and evaluated for the PCs percentage in the GSE.

2.9 Antibacterial activity

The GSE-SOLU solid dispersion was tested for antimicrobial activity by agar well diffusion method against pathogenic bacteria *Proteus sp*, *Staphylococcus aureus*, *Escherichia coli* and *Bacillus sp*. Luria Bertani Agar medium was used to cultivate bacteria. The agar plate surface is inoculated by spreading a volume of the microbial inoculum over the entire agar surface. Fresh overnight culture of each strain was swabbed uniformly onto the individuals plates using sterile cotton swabs. Then, a hole with a diameter of 6 mm is aseptically punched with a sterile borer and a measured volume of the GSE-SOLU at desired concentration is introduced into the well. 3 wells were made on each Luria Bertani Agar plates. Then the centrifuged solution 5 μl of streptomycin (standard), pure GSE, GSE-SOLU solid dispersion, were poured into each well on all plates and incubated for 24 h at 37°C. After incubation the different levels of zonation formed around the well was measured.

2.10 *Antioxidant Assays*

2.10.1 *DPPH free radical scavenging assay*

The antioxidant potential was studied on DPPH free radical. The stock solution for this assay was made by mixing 50 μg of the freeze-dried powder in methanol. Various concentrations of the stock solutions were mixed with 450 μl of Tris-HCl buffer (50 mM-pH 7.4) and free radical DPPH (0.1 mM) in methanol. The mixture was vigorously shaken and it was kept in the dark

for 20 min. After 30 min of incubation, the decrease in the DPPH free radicals was measured at 517 nm. The scavenging activity of GSE, GSE-SOLU formulations were calculated by the following formula,

$$\%\ \text{Scavenging Activity} = \frac{\text{Absorbance of Control}}{\text{Absorbance of Test Sample}} \times 100$$

2.10.2 *ABTS scavenging activity*

Arnao et al method was used for evaluating the ABTS radical scavenging activity [23]. ABTS solution (7.4 mM) was added to potassium persulphate solution (2.6 mM) in equal amounts and the solution was kept for 12 h in the dark at 25˚C. This was referred to as the stock solution. The stock solution was diluted again by addition of ABTS solution; 1 ml in 50 mL of methanol and the absorbance was measured by UV spectrophotometer at 734 nm. For each assay, a freshly prepared ABTS solution was used. ABTS solution and the samples with different concentrations were mixed together and kept at room temperature in dark for 2 h. Methanol was used as blank instead of ABTS solution and the samples absorbance were measured at 734 nm. The scavenging activity was calculated by Trolox equivalents (TE) / ml of the proanthocyanidins.

2.10.3 *FRAP assay*

The ability of the GSE-SOLU formulations, GSE and SOLU to reduce ferrous ions was estimated by Oyaizu method [24]. Phosphate buffer (0.2 M- pH 6.6) and potassium ferricyanide (2.5 ml) mixed with various concentrations of formulations (1 % w/v) and kept in incubator for 30 min at 50 °C. After incubation, 10 % w/v trichloroacetic acid (2.5 ml) was mixed to the above solution and treated as stock solution. 2.5 ml of stock solution was added to 0.1 % w/v

ferric chloride (0.5 ml) and distilled water (2.5 ml) and it is allowed to react for 10 min. Then, the absorbance of the samples was evaluated by a UV-VIS spectrophotometer at 700 nm.

2.10.4 *Lipid peroxidation inhibition*

The inhibitory activity of GSE, SOLU and GSE-SOLU formulations was measured using the Osawa and Namiki [25] method. Linoleic acid (0.13 ml), 50 mM phosphate buffer (10 ml-pH 7.0) and 99.5 % ethanol (10 ml) were dissolved in different concentrations of sample and the volume was made up with distilled water to 25 ml. Each mixture was subjected to incubation for 5 days at 40 ^{o}C in dark. Ferric thiocyanate method was used to measure the degree of oxidation. The incubated mixture (0.1 ml) was added to 20 mM of 0.1 ml ferrous chloride, 30 % of 0.1 ml of ammonium thiocyanate and 75 % ethanol (4.7 ml) solution and incubated for 3 mins. After incubation, the inhibition of peroxide formation was evaluated at 500 nm. The scavenging activity was calculate by;

$$\%\ Lipid\ PeroxideInhibition = 1 - \frac{\text{Absorbance of Sample}}{\text{Absorbance of Control}} \times 100$$

2.11 In-vitro cytotoxicity study

In-vitro cytotoxicity of Pure GSE, SOLU and GSE-SOLU nanodispersion were evaluated by measuring the viability of HCT-116 cells in the presence of different concentrations of nanodispersion. Cell viability was determined by MTT assay (3-(4, 5-dimethylthiazol-2-yl)-2, 5-diphenyltetrazolium bromide). After plating for about 24 hrs, different amounts of GSE, SOLU and GSE-SOLU nanodispersion which are suspended in the culture medium were added in the wells. After incubating at 37°C for 24 hrs, MTT solution (100 µL) were added into each well and incubated for 3 h. MTT is cleaved by mitochondrial succinate dehydrogenase and reductase of viable cells which yields a measurable purple product formazan. The production of formazan is proportional to the viable cell number and inversely proportional to the degree

of cytotoxicity. Then each of the prepared sample solution was read on a Lark LIPR-9608 microplate reader at a wavelength of 540 nm. The cytotoxicity and the biocompatibility of the nanodispersion were stated as % cell viability. It was calculated from the ratio between the number of cells treated with the nanodispersion and that of control (non-treated cells)[26].

3. Results and discussion

3.1 *Optimisation of GSE loading*

Several presentations of GSE-SOLU were formulated with different ratios of SOLU loading, i.e., 1 %, 3 %, 5 % and 7 % of polymer to examine the accurate percentage of GSE in SOLU matrix. Table 1 shows that initial SOLU loading affected the particle size distribution significantly ($p < 0.05$). It is clearly shown that an increase in SOLU loading from 1 % to 5 % resulted in a decrease in the particle size of the formulation. Subsequently, the particle size of the formulation increased as SOLU loading was further increased to 7 %. The 5 % SOLU loading produced a highly stable formulation with highest loading efficacy of about 95.36 % ± 2.06 % and negative zeta potential (-82.1 ± 1.07). The particle size of the FIII formulation was found to be the smallest particle size (69.90 ± 2.12 nm) with PDI of 0.154 ± 0.023. FIII formulation showed the highest loading and stability and therefore, it was selected for further physicochemical analysis.

3.2 *Fourier transform infrared (FT-IR) spectroscopy*

Fig. 2(a) shows the FTIR spectra of SOLU, GSE and FIII dispersion. SOLU displayed a broad peak at 3613 cm^{-1} which can be attributed to O−H vibrational stretching. The peaks at 2914 cm^{-1}, 1737 cm^{-1} and 1627 cm^{-1} are attributed to C−H stretching, C=O and N-H bending vibration respectively. The ether C−O−C has a characteristic peak at 1443 cm^{-1}. GSE show characteristic bands representing O-H stretching at 3319 cm^{-1}, C-C stretching at 1590 cm^{-1} and C-O stretching at 1094 cm^{-1}. The position of the carbonyl peak in the dispersion SOLU- GSE

(FIII) was shifted to 1737.93 cm^{-1} and this shifting led to polar-polar interactions. The FIII formulation, also show a peak broadening from 3619 cm^{-1} to 3265 cm^{-1} indicating an intermolecular hydrogen bonding between GSE and SOLU. The interaction between soluplus and GSE is hydrogen bonding, which results in the shifting and peak broadening of the absorption bands at the interacting functional groups on the FT-IR. The observed FT-IR results are well corroborated with the reports of Dian et al and Bakshi et al [27, 28].

3.3 *X-ray diffraction study*

The diffraction pattern in Fig. 2(b) for the neat SOLU and GSE show broad peaks at 20 and 22, indicating their amorphous nature. The addition of SOLU to the GSE completely eliminate the broad peak, indicating a hydrogen bonding and a π-π interactions between GSE and SOLU molecules. The FIII formulation showed no characteristic peak which indicated that GSE was completely amorphous. Soluplus has been demonstrated to retard and inhibit the crystallization, giving amorphous solid dispersions. A similar result has been previously reported by Shamma et al [29] on carvedilol-SOLU dispersion.

3.4 *AFM Analysis*

The surface topography of the prepared GSE-SOLU dispersion was studied with atomic force microscopy. The pure SOLU exhibited a sheet-like morphology (Fig. 3(a) while GSE is spherical in shape (Fig. 3(b). As shown in Fig 3(c-f), the GSE-SOLU formulations (FI-FIV) show particles that are dispersed in the polymer matrix. In the FI formulation, the particle size is deformed and very large. The GSE-SOLU dispersion in the FII formulation show agglomeration with less distribution over the polymer surface. The FIII formulation displays particles with relatively uniform size distribution throughout the polymer matrix. The FIV formulation micrographs clearly demonstrated a highly crosslinked morphology with increase aggregates over the polymer matrix. Liu et al reported that the proanthocyanidins-Insulin

hybrid nanoparticles showed a controlled morphology with spherically shaped particles. They also mentioned that medium concentration showed good stability to form uniform sized particles [30]. The surface roughness data is displayed in Fig. 3 (g-l). The AFM 3D surface imaging study of GSE-SOLU formulations help us to understand the surface morphology of GSE-SOLU and their interactions. The AFM images indicates the amorphous nature of GSE in the SOLU of the dispersions and showed high surface interaction. Bhagel *et al*., revealed that SOLU showed uniform distribution and stability of the dispersion. Therefore the results are similar with the reports of Bhagel et al and Fule et al [31, 32].

3.5 *SEM Analysis*

SEM images of GSE and the FIII formulations were used to examine their morphological changes Fig 4. Fig 4(b) reveals that GSE exists as spherically shaped smooth surfaced particles and SOLU (Fig 4(a) appears to be thin flat sheet-like in appearance. The FIII formulation exhibited a homogenous dispersion in which the spherically shaped particles of GSE (Fig 4(c) & (d)).

3.6 *TEM Analysis*

The morphology of the SOLU, GSE, FIII GSE-SOLU dispersions and the selected area diffraction pattern (SAED) of FIII freeze-dried formulation are shown in Fig 4. From the micrographs, it is evident that SOLU (Fig 4(e)) has a flat thin sheet-like morphology, GSE (Fig 4(f)) appears to have a spherically shaped structure and in Fig 4(g) it is clear that the spherically shaped particles of GSE are embedded on the surface of the polymer which has a thin flat sheet-like morphology. The freeze-dried solid dispersion FIII (Fig 4(g)) show that the spherically shaped particles of GSE are well distributed in the polymer matrix. The SAED image (Fig 4(h)) show the absence of the diffused rings which confirms the amorphous nature of the freeze-dried solid dispersion.

3.7 *In-vitro release*

The controlled release behaviour of PCs is shown in Fig 5. The release of PCs decreases with increase in polymer content. The results show that the PCs release at pH 6.8 from SOLU may be due to the formation of pores after the swelling of the polymer. Dissolution profiles of formulations FIII show a lower burst effect with 20.00 % dissolved after 2 h and the final concentration was about 68.05 % after 48 h. Thus, it is evident that the increased polymer ratio was responsible for the decreased dissolution rate and lower burst effect. The hydrophobic ability of the polymer was greater than its hydrophilic capability. When SOLU was blended with PCs, the interaction or affinity between the polymer and SOLU might be enhanced and thus caused the slower release. The pure GSE from the solution exhibited about 97.33 % release in 2 h. FIII formulation containing GSE-SOLU suspension displayed a controlled release behaviour and the release at 48 h was 68.05%[33]. The inset in the Fig 3 shows that about 45-50 % of GSE was released in 6 h. The amount of proanthocyanidins in ethanol solutions depends on the percentage of ethanol in the medium. The presence of ethanol in the gastrointestinal tract didn't cause any alterations in the dissolution but the dissolution profile was found to be very less compared to SIF. The *in-vitro* release of proanthocyanidins in water shows a comparable dissolution behaviour as that of SIF. Similar result had been reported in Lu *et al's* work for the procyanidins release in tea after 6 h [34].

3.8 Antibacterial activity

The antimicrobial activity of standard (erythromycin), GSE and GSE-SOLU solid dispersion was tested using the agar well diffusion method (Fig 6A). The zone of inhibition as seen in Fig 6B showed the range of 3-6 mm for standard, 5-8.5 mm for GSE and 9-13 mm for GSE-SOLU solid dispersion (FIII). The result of the present investigation highlights the greater antibacterial potential of the solid dispersion than for the pure GSE and the standard drug. The higher antimicrobial activity of GSE-SOLU solid dispersion may be because of the amphiphilic

nature of SOLU which interacts with the cell membrane of the bacterial cell wall to release the GSE promptly from the solid dispersion. Nirmala et al studied the antimicrobial activities of GSE (10 µl) and they found the zone of inhibition in the range of 8-16 mm [35]. In our study we have obtained similar results by using only 5 µl of the samples and found good antibacterial activity with a zone of inhibition of 9-13 mm[33].

3.9 *Antioxidant Activity*

3.9.1 *DPPH*

The electron (hydrogen) donating ability of GSE, SOLU and GSE-SOLU formulations were measured. The reaction between DPPH and the antioxidants gave an estimation of the scavenging ability. The DPPH solution was purple in colour and upon addition of the GSE-SOLU formulations, it became colourless. This discolouration indicates a higher scavenging capacity via donation of the proanthocyanidins hydrogen to the free radicals. In addition, the GSE and the GSE-SOLU formulations exhibited an increase in scavenging the free radicals with an increase in concentration.

The scavenging activity of different concentrations of GSE and GSE-SOLU formulations are shown in Fig 7(b). When the concentration of GSE-SOLU formulation (FIII) was increased to 200 µg/ml, it displayed the highest scavenging ability of about 96.09 % when compared with GSE. The presence of a functional group –OH and a flavonoid moiety in the proanthocyanidins performs the scavenging activity against the free radicals such as hydroxyl, superoxide, DPPH and a reduction in the formation of hydrogen peroxide (Fig 7(a)). Moreover, the reason for higher antioxidant activity could be due to the presence of monomeric, dimeric and oligomeric proanthocyanidins [36]. Arora et al., also reported that the antioxidant ability can be determined by the presence of a functional group and the position of proanthocyanidin molecule [37].

The data presented in Fig 7 were analyzed to evaluate the % inhibition of DPPH of GSE and GSE-SOLU formulations (FI-FIV). A Calibration curve was created by plotting the concentrations of GCE and GSE-SOLU formulations against DPPH scavenging activity. The corresponding R^2 values showed the % antioxidant activity. The activity of pure GSE showed the R^2 value of 0.95925, FI-0.90647, FII-0.95017, FIII-0.97628 and FIV-0.95132 (Fig 8). From the R^2 values, it was found that the equimolar concentration of GSE-SOLU formulations and pure GSE have similar scavenging ability. This confirms the protection of complete functional moiety of GSE when dispersed with the SOLU matrix.

3.9.2 *ABTS radical scavenging activity*

The antioxidant ability of GSE, GSE-SOLU formulations was tested against long shelf life radical ABTS. They formed an intense coloured solution when ABTS reacted with oxidants and peroxyl radicals. The scavenging activity was measured by the ability of GSE and GSE-SOLU formulations in decreasing the colour intensity. When they reacted with radical anion ABTS. This radical scavenging assay could be used to measure both the hydrophobic and hydrophilic antioxidants because the reagents used in this method acted well in both types of antioxidants. Table 2 shows the ABTS radical scavenging activity of GSE and GSE-SOLU formulations. The antioxidant activity of GSE and GSE-SOLU show increased activity as the concentration increased but the activity varies with the pure GSE and GSE-SOLU formulations. Hence, both the GSE and GSE-SOLU formulations exhibited a dose-dependent scavenging activity. In addition, there was no significant difference in the antioxidant activity when the concentration was increased from 120 to 200 µg/ml ($p > 0.05$). Our results corroborated well with the work reported by Sofi et al and Selcuk et al [38, 39]. The dose-dependent activity is due to the presence of hydroxyl groups, number of aromatic rings in the chemical structure and molecular weight of the molecule [40]. The formulations exhibited a strong antioxidant activity because the polymer SOLU also acts as an antioxidant along with

414 the GSE. The results suggest that the formulation was found to be a strong ABTS radical
415 inhibitor when compared with GSE.
416
417 **3.9.3** ***FRAP assay***
418 It was found that the reducing ability of GSE and GSE-SOLU formulations could make them
419 acts as good antioxidants. In FRAP assay, we measured the reduction of ferric (Fe^{3+}) 2, 4, 6
420 tripyridyl-5-triazine (TPTZ) to a ferrous (Fe^{2+}) product. During the reduction, the Fe^{2+} showed
421 the formation of Perl's Prussian blue colour. Table 2 shows the reducing capacity of GSE and
422 GSE-SOLU formulations at different concentrations. The reducing capacity of GSE and GSE-
423 SOLU formulations increased when the concentration increased. When compare with all the
424 other formulations, FIII and FIV show the highest reducing power. The highest reducing power
425 of the FIII and FIV formulations can be attributed to the presence of many hydroxyl groups in
426 their structure and the polymer (SOLU).
427
428 **3.9.4** ***Linoleic acid emulsion system assay***
429 The quality of food commodities is affected by several factors. Among these, lipid auto-
430 oxidation is one of the most undesirable factors that can deteriorate the food and food
431 components. The importance of protecting the food against oxidative damage has prompted the
432 wider usage of antioxidants from natural origin. Rancidity occurs due to the rapid development
433 of lipid peroxidation and it is measured as a main mechanism of quality deterioration in lipids.
434 GSE and GSE-SOLU formulations prevented the lipid peroxidation by means of free radical
435 scavenging and electron transfer mechanisms. During the processing of lipid foods, these
436 antioxidants can be added to suppress lipid peroxidation, to improve the stability and quality
437 of the food product. And also, the lipid peroxidation of the cellular membrane causes
438 pathological illness which leads to atherosclerosis, inflammation and other diseases. The
439 reducing property of GSE-SOLU formulation indicates that they can be used as electron donors

which reduces lipid peroxidation processes [41]. The main mechanism in this assay is that the polymer SOLU protects the GSE and slowly releases the electron from the proanthocyanidins to scavenge the harmful peroxidase radical. This property increases the operational stability and shielding effect of PEG-PCL-PVA (SOLU) in scavenging peroxidase radical. The percentage of lipid peroxidase inhibition showed increased activity in the GSE-SOLU formulations compared with GSE (Table 2). This indicates that SOLU does not only possess antioxidant activity but also increases the stability of the formulations [42].

3.10 *In-vitro* cytotoxicity

The GSE used in this study contains only proanthocyanidins and in addition, there are no reported studies on the controlled release formulation of solid dispersions containing proanthocyanidins and SOLU. To determine the cytotoxic activities of pure GSE and GSE-SOLU solid dispersion, studies were performed on human colon cancer cells by MTT assay. The fabricated system did not exhibit any cytotoxicity to the normal cells during the analysis, confirming that the SOLU act merely as a suitable vehicle for proanthocyanidins. The SOLU in a concentration of 200 μg/mL were treated with the cells and subjected for 24 h incubation. They showed cell viability above 96%, indicating that the synthesized hybrid system were highly biocompatible with the colon cells. Hence it was concluded that the nanoparticles themselves did not have any harmful effects on living cells. This clearly revealed their safe application inside the body during proanthocyanidins delivery (Fig 9).

4. Conclusions

GSE was successfully dispersed on the soluplus matrix using the freeze-drying method with a loading efficiency of 95.36 %. The mean diameter of GSE-SOLU dispersion was ~69.90 and PDI of 0.154. The FT-IR analysis indicates an intermolecular hydrogen bonding between the GSE and SOLU. The morphological analysis proved that spherically shaped particles of GSE

are well distributed in the polymer matrix. In this study, GSE-SOLU formulations were screened for antioxidant property. *In-vitro* antioxidant assays showed that the functional property of GSE was protected after dispersion into the polymer matrix. The study also revealed that GSE and SOLU possess higher hydroxyl group emphasizing its impact in the *in-vitro* anti-oxidative activity assays. Therefore, it can be recommended that the GSE-SOLU be used as a promising antioxidant compound in the food industry. The results of the present work denotes that GSE constitutes a good source of PC's and will be useful in the prevention and treatment of free radical related diseases. In addition, the resultant GSE-SOLU dispersion could also be used as an antioxidant in many applications such as antidiabetic, anticancer, anti-inflammatory and in wound healing applications.

Acknowledgements: The authors wish to express their sincere thanks to the DST-Inspire Fellowship, Department of Science and Technology, New Delhi for their financial support. This study was also financially supported by Project "Agropreparations of the new generation: a strategy of construction and realization" (Agreement No 074-02-2018-328) in accordance with Resolution No 220 of the Government of the Russian Federation of April 9, 2010, "On measures designed to attract leading scientists to the Russian institutions of higher learning".

Ethical standards

The manuscript does not contain clinical studies.

Conflict of interest

The authors declare no conflict of interest.

References

[1] Delgado Adámez, J.; Gamero Samino, E.; Valdés Sánchez, E.; González-Gómez, D. In

Vitro Estimation of the Antibacterial Activity and Antioxidant Capacity of Aqueous Extracts from Grape-Seeds (Vitis Vinifera L.). *Food Control*, **2012**, *24* (1–2), 136–141. https://doi.org/10.1016/j.foodcont.2011.09.016.

[2] Songsermsakul, P.; Pornphairin, E.; Porasuphatana, S. Comparison of Antioxidant Activity of Grape Seed Extract and Fruits Containing High β-Carotene, Vitamin C, and E. *Int. J. Food Prop.*, **2013**, *16* (3), 643–648. https://doi.org/10.1080/10942912.2011.561462.

[3] Katalinić, V.; Možina, S. S.; Skroza, D.; Generalić, I.; Abramovič, H.; Miloš, M.; Ljubenkov, I.; Piskernik, S.; Pezo, I.; Terpinc, P.; et al. Polyphenolic Profile, Antioxidant Properties and Antimicrobial Activity of Grape Skin Extracts of 14 Vitis Vinifera Varieties Grown in Dalmatia (Croatia). *Food Chem.*, **2010**, *119* (2), 715–723. https://doi.org/10.1016/j.foodchem.2009.07.019.

[4] Subbaiya, R.; Lavanya, R. S.; Selvapriya, K.; Selvam, M. M. Original Research Article Green Synthesis of Silver Nanoparticles from Phyllanthus Amarus and Their Antibacterial and Antioxidant Properties. **2014**, *3* (1), 600–606.

[5] Ma, Q.; Ren, Y.; Wang, L. Investigation of Antioxidant Activity and Release Kinetics of Curcumin from Tara Gum/ Polyvinyl Alcohol Active Film. *Food Hydrocoll.*, **2017**, *70*, 286–292. https://doi.org/10.1016/j.foodhyd.2017.04.018.

[6] Nagaich, U.; Gulati, N.; Chauhan, S. Antioxidant and Antibacterial Potential of Silver Nanoparticles: Biogenic Synthesis Utilizing Apple Extract. *J. Pharm.*, **2016**, *2016*, 1–8. https://doi.org/10.1155/2016/7141523.

[7] From, A. B.; Hills, K.; Ghats, E.; Tamilnadu, O.; Sathish, S. S.; Vimala, A.; Kanaga, A.; Murugan, M. Antioxidant and Antimicrobial Studies on Biosynthesized Silver Nanoparticles Using Bryum Medianum Mitt . **2016**, *8* (1), 704–709.

[8] Mandic, A. I.; Đilas, S. M.; Ćetković, G. S.; Čanadanović-Brunet, J. M.; Tumbas, V. T. Polyphenolic Composition and Antioxidant Activities of Grape Seed Extract. *Int. J.*

Food Prop., **2008**, *11* (4), 713–726. https://doi.org/10.1080/10942910701584260.

[9] Cos, P.; De Bruyne, T.; Hermans, N.; Apers, S.; Berghe, D. Vanden; Vlietinck, a J. Proanthocyanidins in Health Care: Current and New Trends. *Curr. Med. Chem.*, **2004**, *11* (10), 1345–1359. https://doi.org/10.2174/0929867043365288.

[10] Santos-Buelga, C.; Scalbert, A. Proanthocyanidins and Tannin like Compounds Nature, Occurrence, Dietary Intake and Effects on Nutrition and Health. *J. Sci. Food Agric.*, **2000**, *80* (May), 1094–1117. https://doi.org/10.1002/(SICI)1097-0010(20000515)80.

[11] Ou, K.; Gu, L. Absorption and Metabolism of Proanthocyanidins. *J. Funct. Foods*, **2014**, *7* (1), 43–53. https://doi.org/10.1016/j.jff.2013.08.004.

[12] Antonacci D, B. M. Anticancer Effects of Grape Seed Extract on Human Cancers: A Review. *J. Carcinog. Mutagen.*, **2014**, *s8* (01), 1–14. https://doi.org/10.4172/2157-2518.S8-005.

[13] Mansouri, E.; Panahi, M.; Ghaffari, M. A.; Ghorbani, A. Effects of Grape Seed Proanthocyanidin Extract on Oxidative Stress Induced by Diabetes in Rat Kidney. *Iran. Biomed. J.*, **2011**, *15* (3), 100–106.

[14] Deeban, A.; Anand, K.; Lakshmi, T. In Vitro Anti Arthritic Activity of Grape Seed Ethanolic Extract. *Int. J. Pharmacogn. Phytochem. Res.*, **2015**, *7* (5), 977–979.

[15] Wu, C. S. Enhanced Antibacterial Activity, Antioxidant, and in Vitro Biocompatibility of Modified Polycaprolactone-Based Membranes. *Int. J. Polym. Mater. Polym. Biomater.*, **2016**, *65* (17), 872–880. https://doi.org/10.1080/00914037.2016.1180605.

[16] Fine, A. M. Oligomeric Proanthocyanidin Complexes : Applications Oligomeric Proanthocyanidins. *Altern. Med. Rev.*, **2000**, *5* (2), 144–151.

[17] Ali, S. Soluplus ® – The Solid Solution Opening New Doors in Solubilization . *BASF Prod. Lit.*, **2012**, 1–8.

[18] Reintjes, T. 10. Kolliphor™ P Grades (Poloxamers). *Solubility Enhanc. with BASF Pharma Polym. Solubilizer Compend.*, **2011**, 103–111.

[19] Vasconcelos, T.; Sarmento, B.; Costa, P. Solid Dispersions as Strategy to Improve Oral Bioavailability of Poor Water Soluble Drugs. *Drug Discov. Today*, **2007**, *12* (23–24), 1068–1075. https://doi.org/10.1016/j.drudis.2007.09.005.

[20] Zsombor K. Nagy, Attila Balogh, Balazs Vajna, Attila Farkas, Grego Patyi, A. K. and G. M. Comparison of Electrospun and Extruded Soluplus-Based Solid Dosage Forms of Improved Dissolution. *J. Pharm. Sci.*, **2012**, *101* (1), 322–332. https://doi.org/10.1002/jps.

[21] Gibis, M.; Rahn, N.; Weiss, J. Physical and Oxidative Stability of Uncoated and Chitosan-Coated Liposomes Containing Grape Seed Extract. *Pharmaceutics*, **2013**, *5* (3), 421–433. https://doi.org/10.3390/pharmaceutics5030421.

[22] Z. Wang, X. Ju, R. He, J. Yuan, R. E. A. Effect of High Pressure Treatment on Rapeseed Protein Microparticle Properties and Gastrointestinal Release Behavior of the Encapsulated Peptides,. *Food Res. Int.*, **2015**, *77*, 549–555.

[23] Arnao, M., Cano, A., & Acosta, M. The Hidrophilic and Lipophilic Contribution to Total Antioxidant Activity. *Food Chem.*, **2001**, *73* (2), 239–244.

[24] Oyazu, M. Studies of Product Browning Reaction: Antioxidant Activity of Producbrowning Reaction from Glucosamine. *Jap. J. Nut*, **1986**, *44*, 315–397.

[25] Osawa, T.; Namiki, M. Natural Antioxidants Isolated from Eucalyptus Leaf Waxes. *J. Agric. Food Chem.*, **1985**, *33* (5), 777–780.

[26] Bahuguna, A.; Khan, I.; Bajpai, V. K.; Kang, S. C. MTT Assay to Evaluate the Cytotoxic Potential of a Drug. *Bangladesh J. Pharmacol.*, **2017**, *12* (2), 115–118. https://doi.org/10.3329/bjp.v12i2.30892.

[27] Dian, L.; Yu, E.; Chen, X.; Wen, X.; Zhang, Z.; Qin, L.; Wang, Q.; Li, G.; Wu, C. Enhancing Oral Bioavailability of Quercetin Using Novel Soluplus Polymeric Micelles. *Nanoscale Res. Lett.*, **2014**, *9* (1), 1–11. https://doi.org/10.1186/1556-276X-9-684.

[28] Bakshi, P.; Sadhukhan, S.; Maiti, S. Design of Modi Fi Ed Xanthan Mini-Matrices for

570 Monitoring Oral Discharge of Highly Soluble Soluplus ® – Glibenclamide Dispersion.
571 *Mater. Sci. Eng. C*, **2015**, *54*, 169–175. https://doi.org/10.1016/j.msec.2015.05.014.
572 [29] Shamma, R. N.; Basha, M. Soluplus®: A Novel Polymeric Solubilizer for Optimization
573 of Carvedilol Solid Dispersions: Formulation Design and Effect of Method of
574 Preparation. *Powder Technol.*, **2013**, *237*, 406–414.
575 https://doi.org/10.1016/j.powtec.2012.12.038.
576 [30] Liu, R.; Wang, L.-B.; Huang, R.-L.; Su, R.-X.; Qi, W.; Yu, Y.-J.; He, Z.-M. Self-
577 Assembled Oligomeric Procyanidin–Insulin Hybrid Nanoparticles: A Novel Strategy for
578 Controllable Insulin Delivery. *Biomater. Sci.*, **2013**, *1* (8), 834.
579 https://doi.org/10.1039/c3bm60066a.
580 [31] Baghel, S.; Cathcart, H.; O'Reilly, N. J. Polymeric Amorphous Solid Dispersions: A
581 Review of Amorphization, Crystallization, Stabilization, Solid-State Characterization,
582 and Aqueous Solubilization of Biopharmaceutical Classification System Class II Drugs.
583 *J. Pharm. Sci.*, **2016**, *105* (9), 2527–2544. https://doi.org/10.1016/j.xphs.2015.10.008.
584 [32] Fule, R.; Amin, P. Development and Evaluation of Lafutidine Solid Dispersion via Hot
585 Melt Extrusion: Investigating Drug-Polymer Miscibility with Advanced
586 Characterisation. *Asian J. Pharm. Sci.*, **2014**, *9* (2), 92–106.
587 https://doi.org/10.1016/j.ajps.2013.12.004.
588 [33] Rajendran, R.; Volova, T.; Oluwafemi, O. S.; S, R.; Thomas, S.; Kalarikkal, N. Nano
589 Formulated Proanthocyanidins as an Effective Wound Healing Component. *Mater. Sci.*
590 *Eng. C*, **2020**, *106* (February 2019), 110056.
591 https://doi.org/10.1016/j.msec.2019.110056.
592 [34] Lu, Q.; Li, D. C.; Jiang, J. G. Preparation of a Tea Polyphenol Nanoliposome System
593 and Its Physicochemical Properties. *J. Agric. Food Chem.*, **2011**, *59* (24), 13004–13011.
594 https://doi.org/10.1021/jf203194w.
595 [35] Grace Nirmala, J.; Narendhirakannan, R. T. In Vitro Antioxidant and Antimicrobial

Activities of Grapes (Vitis Vinifera. L) Seed and Skin Extracts - Muscat Variety. *Int. J. Pharm. Pharm. Sci.*, **2011**, *3* (4), 242–249.

[36] Saito, M.; Hosoyama, H.; Ariga, T.; Kataoka, S.; Yamaji, N. Antiulcer Activity of Grape Seed Extract and Procyanidins. *J. Agric. Food Chem.*, **1998**, *46* (4), 1460–1464.

[37] Arora, A.; Nair, M. G.; Strasburg, G. M. Structure–Activity Relationships for Antioxidant Activities of a Series of Flavonoids in a Liposomal System. *Free Radic. Biol. Med.*, **1998**, *24* (9), 1355–1363.

[38] Sofi, F. R.; Raju, C. V.; Lakshmisha, I. P.; Singh, R. R. Antioxidant and Antimicrobial Properties of Grape and Papaya Seed Extracts and Their Application on the Preservation of Indian Mackerel (Rastrelliger Kanagurta) during Ice Storage. *J. Food Sci. Technol.*, **2016**, *53* (1), 104–117. https://doi.org/10.1007/s13197-015-1983-0.

[39] Selcuk, A. R.; Demiray, E.; Yilmaz, Y.; Kelimeler, A.; Aktivite, A. Antioxidant Activity of Grape Seeds Obtained from Molasses (Pekmez) and Winery Production. *Akad. Gıda*, **2011**, *9* (5), 39–43.

[40] Spigno, G.; De Faveri, D. M. Antioxidants from Grape Stalks and Marc: Influence of Extraction Procedure on Yield, Purity and Antioxidant Power of the Extracts. *J. Food Eng.*, **2007**, *78* (3), 793–801. https://doi.org/10.1016/j.jfoodeng.2005.11.020.

[41] Jayaprakasha, G. K.; Singh, R. P.; Sakariah, K. K. Antioxidant Activity of Grape Seed (Vitis Vinifera) Extracts on Peroxidation Models in Vitro. *Food Chem.*, **2001**, *73* (3), 285–290. https://doi.org/10.1016/S0308-8146(00)00298-3.

[42] Piao, J.; Lee, J. Y.; Bae, J. W.; Ma, C. J.; Ko, H. J.; Kim, D. D.; Kang, W. S.; Cho, H. J. Angelica Gigas Nakai and Soluplus-Based Solid Formulations Prepared by Hot-Melting Extrusion: Oral Absorption Enhancing and Memory Ameliorating Effects. *PLoS One*, **2015**, *10* (4), 1–19. https://doi.org/10.1371/journal.pone.0124447.

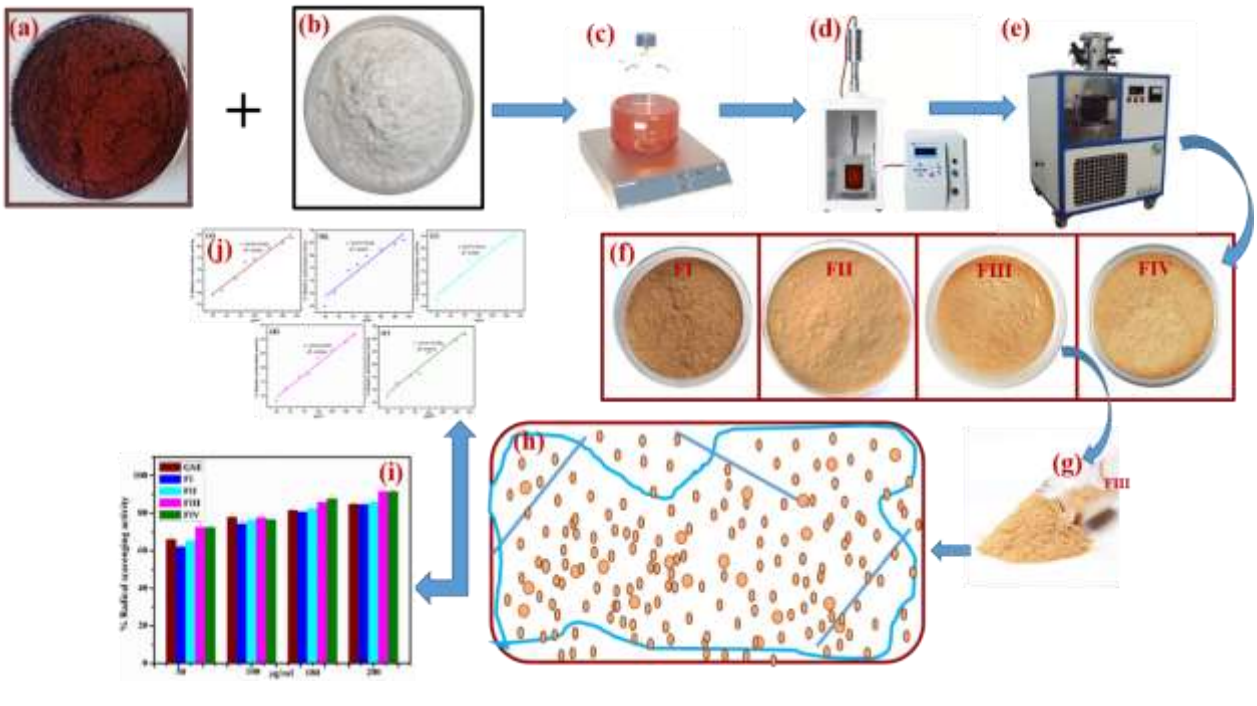

Graphical Abstract: Process of GSE-SOLU dispersion and its antioxidant activity (a) Grape seed extract (b) Soluplus (c) Mixing of GSE and SOLU using magnetic stirrer (d) Probe sonication (e) Lyophilisation (f) Lyophilised powder (GSE-SOLU dispersions) (g) FIII formulation for further studies (h) Morphology showing uniform dispersion of GSE in the SOLU matrix (i) Antioxidant activity (j) DPPH calibration curve

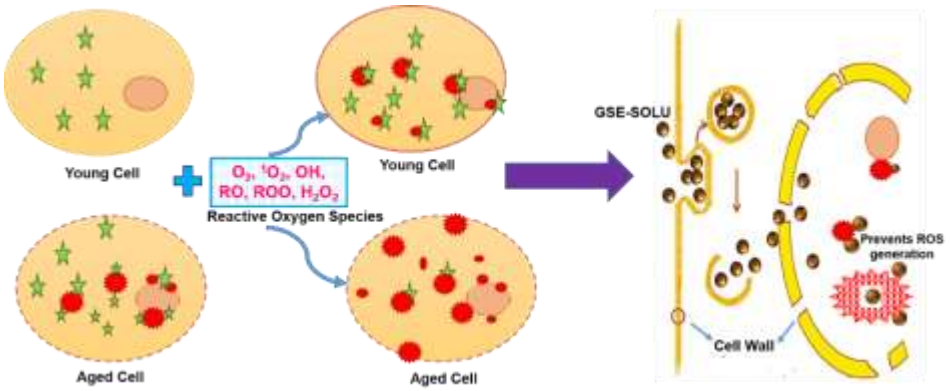

Fig. 1 Mechanism of antioxidant system

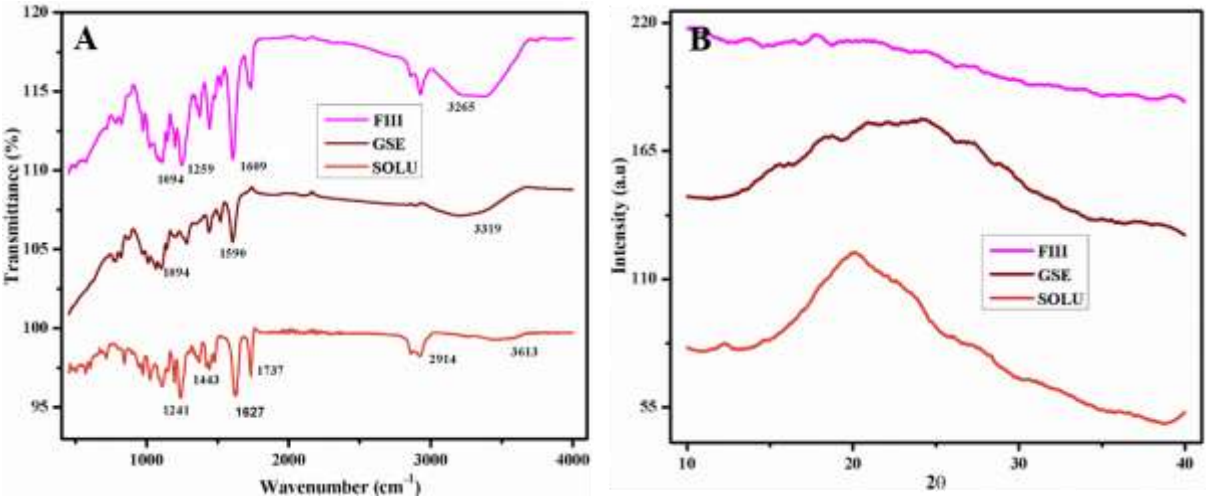

Fig 2 (A) FTIR spectra of SOLU, GSE and FIII dispersion and (B) X-ray diffractograms of SOLU, GSE and FIII dispersion

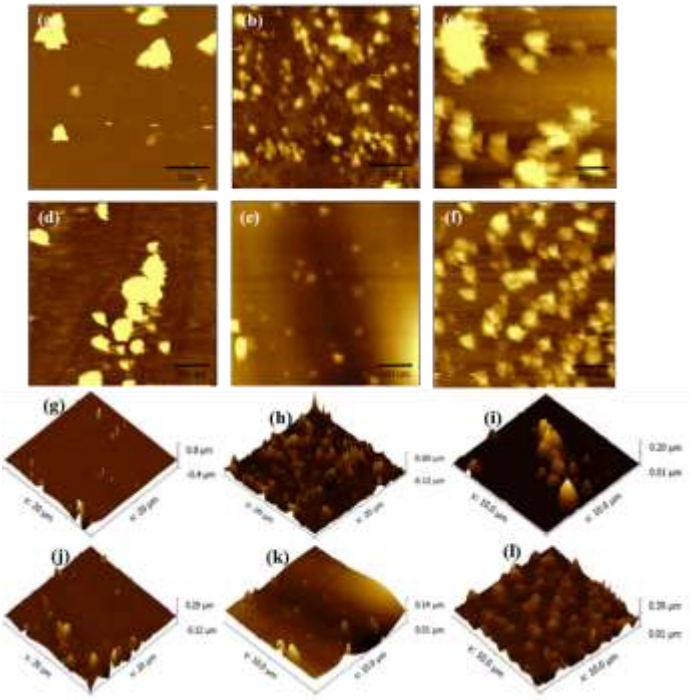

Fig. 3 AFM images of (a) SOLU, (b) GSE, (c) FI, (d) FII, (e) FIII, (f) FIV GSE-SOLU dispersions, 3D AFM images of (g) SOLU, (h) GSE, (i) FI, (j) FII, (k) FIII, (l) FIV GSE-SOLU dispersions

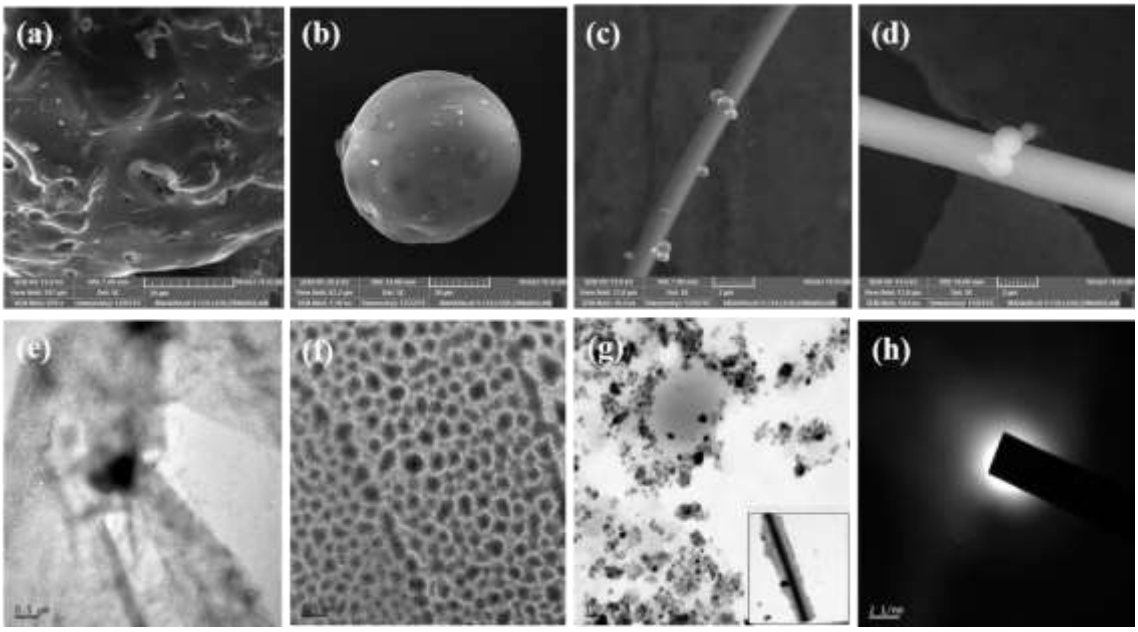

Fig. 4 SEM images of (a) SOLU, (b) GSE and (c) & (d) GSE-SOLU (FIII) dispersion and TEM images of (e) SOLU (0.5 µm), (f) GSE (0.5 µm), (g) GSE-SOLU (FIII) dispersion (100 nm) and (h) SAED pattern of GSE-SOLU dispersion

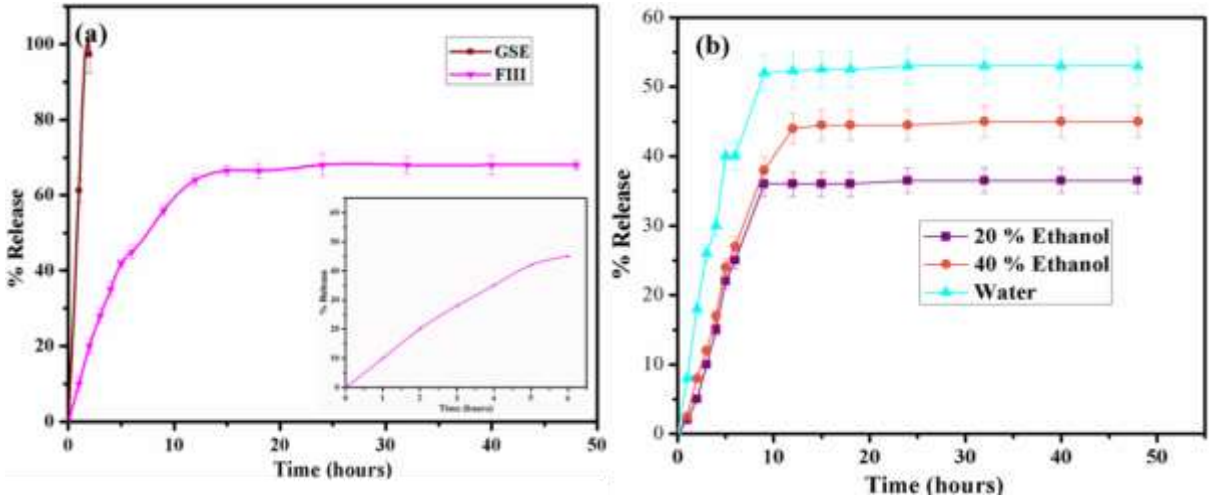

Fig 5 *In-vitro* release of GSE and FIII formulation in (a) SIF and (b) Ethanol (20 % & 40 %), Water

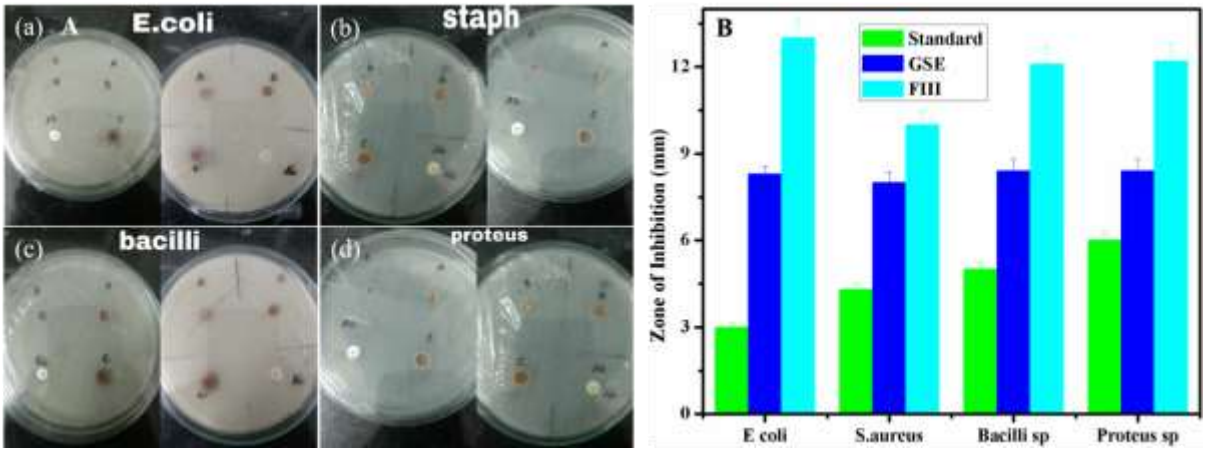

665 **Fig 6: (A) Photographs showing the agar well diffusion method of standard (A), GSE (B)**
666 **and GSE-SOLU (FIII) solid dispersion (C), (B) Antibacterial Activity of standard, GSE**
667 **and GSE-SOLU (FIII) solid dispersion against *E.coli*, *S.aureus*, *Bacillus sp* and *Proteus***
668 ***sp.***

669

670

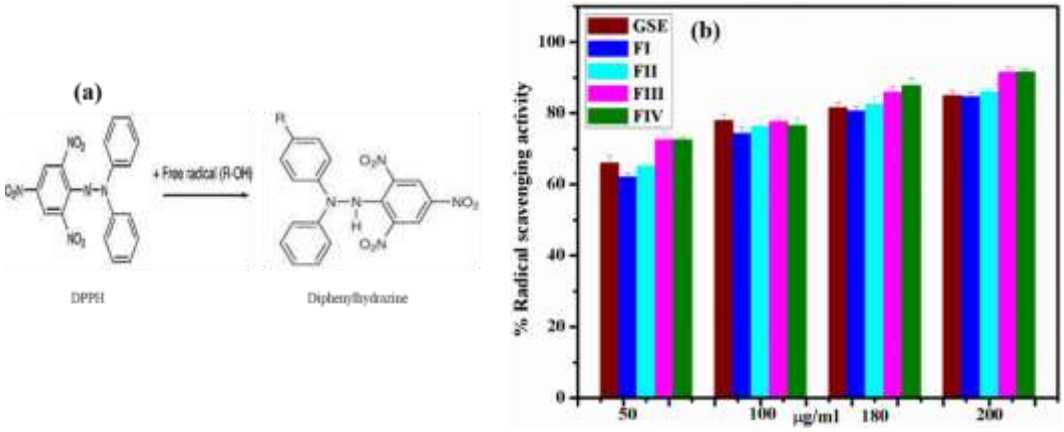

671

672 **Fig. 7 (a) Molecular representation of antioxidant mechanism of DPPH, (b) Antioxidant**
673 **activity of GSE and formulations FI, FII, FIII & FIV at different concentrations**

674

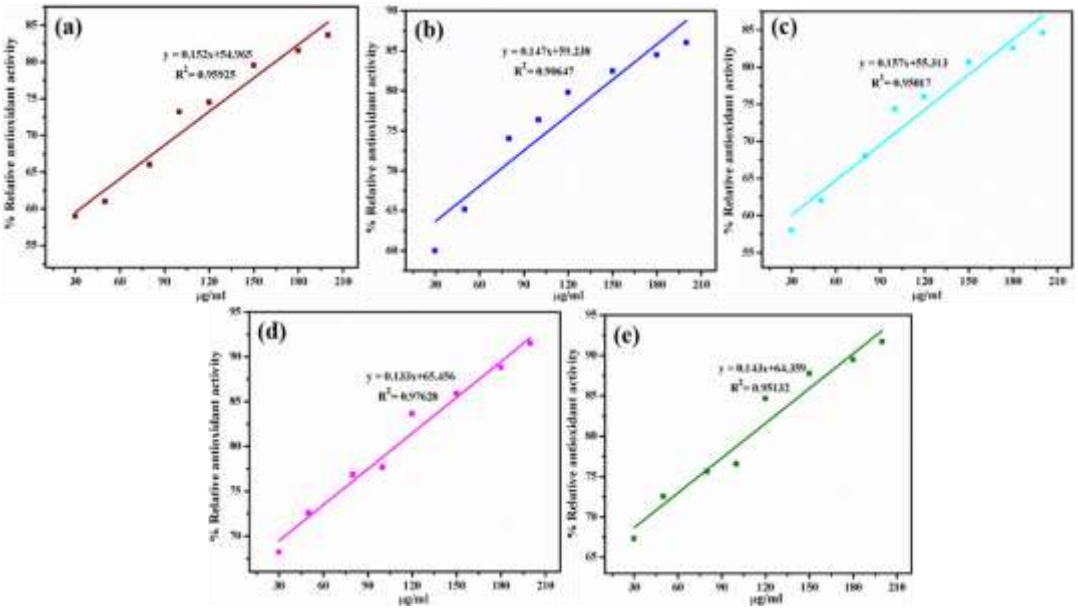

Fig. 8 DPPH calibration curve of GSE and its formulations. This was obtained by plotting various amounts of GSE (a), FI (b), FII (c), FIII (d) & FIV (e) formulations (µg/ml) vs. % inhibition of DPPH

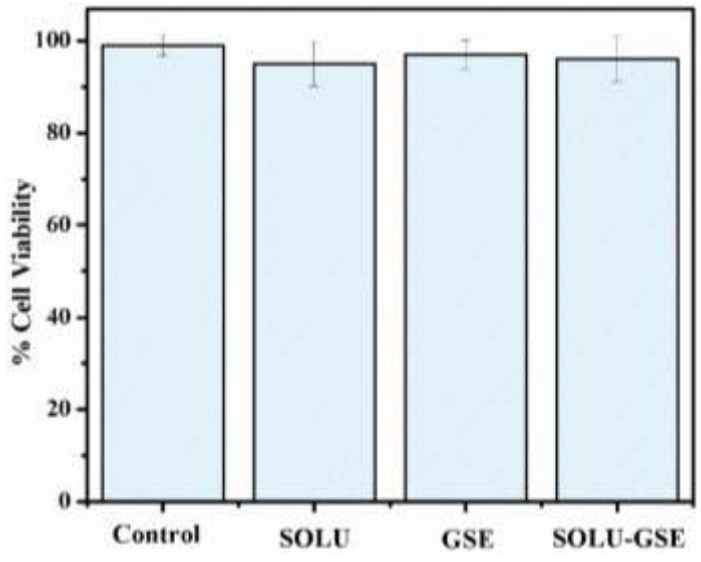

Fig. 9 Cell viability upon incubation with SOLU, PCs and PCs-SOLU for 24 h as determined by MTT assay.

689 **Table 1 Effects of GSE loading on Size, PDI, ZP and LE**

Formulations	SOLU loading (%)	Size (nm)	PDI	ZP (mV)	LE (%)
FI	1	377.9 ± 3.78	0.184 ± 0.024	-46.8 ± 1.04	87.16 ± 2.04
FII	3	275.5 ± 1.54	1.761 ± 0.042	-48.4 ± 1.24	92.58 ± 2.45
FIII	5	69.90 ± 2.12	0.154 ± 0.023	-82.1 ± 1.07	95.36 ± 2.06
FIV	7	75.80 ± 2.17	0.410 ± 0.031	-43.3 ± 1.00	80.41 ± 3.74

690 **PDI-Poly dispersity index; ZP-Zeta potential; LE-Loading efficiency**

691

692 **Table 2 Antioxidant activity of GSE and GSE-SOLU Formulations**

ABTS radical scavenging					
µg/ml	**GSE**	**FI**	**FII**	**FIII**	**FIV**
30	20.54 ± 1.27	21.14 ± 2.40	19.65 ± 1.65	24.25 ± 1.64	22.38 ± 2.31
50	26.59 ± 2.40	25.21 ± 2.80	24.89 ± 1.89	32.15 ± 1.89	28.57 ± 3.21
80	310.00 ± 2.09	307.14 ± 2.45	302.78 ± 1.64	312.67 ± 2.64	311.44 ± 3.14
100	587.32 ± 2.54	579.14 ± 1.58	565.55 ± 2.58	590.28 ± 2.14	594.32 ± 2.98
120	597.34 ± 2.92	584.47 ± 1.98	576.32 ± 2.34	600.47 ± 1.67	599.68 ± 2.64
150	610.21 ± 2.45	592.31 ± 2.38	586.34 ± 1.98	617.24 ± 2.49	615.87 ± 2.70
180	612.84 ± 1.98	607.47 ± 2.84	586.34 ± 2.35	619.58 ± 1.37	618.47 ± 2.45
200	617.53 ± 1.68	611.56 ± 2.31	586.34 ± 2.86	625.34 ± 2.44	626.42 ± 2.31
Ferric reducing antioxidant power					
µg/ml	**GSE**	**FI**	**FII**	**FIII**	**FIV**
50	0.25 ± 0.84	0.18 ± 0.82	0.2 ± 1.15	0.28 ± 1.11	0.27 ± 0.89
100	0.38 ± 1.2	0.24 ± 1.00	0.29 ± 1.65	0.40 ± 1.45	0.38 ± 1.09
150	0.57 ± 1.1	0.45 ± 1.45	0.49 ± 1.42	0.58 ± 1.21	0.58 ± 1.16
180	0.75 ± 1.4	0.64 ± 1.20	0.68 ± 1.87	0.78 ± 1.01	0.78 ± 1.54
200	0.88 ± 1.1	0.75 ± 1.70	0.84 ± 1.24	0.90 ± 0.98	0.87 ± 1.24
Lipid peroxidation inhibition					
µg/ml	**GSE**	**FI**	**FII**	**FIII**	**FIV**
100	47.45 ± 0.85	67.69 ± 0.87	70.00 ± 1.01	72.04 ± 1.06	73.00 ± 1.05
200	52.18 ± 0.56	74.22 ± 1.24	75.24 ± 1.58	78.41 ± 0.98	76.87 ± 1.31
500	66.14 ± 1.20	81.27 ± 1.14	83.21 ± 1.07	86.58 ± 1.21	87.24 ± 1.05

693

694

695

696